archives
of thermodynamics
Vol. **38**(2017), No. 1, 39–62
DOI: 10.1515/aoter-2017-0003

Thermodynamic analysis of a new dual evaporator CO_2 transcritical refrigeration cycle

EZZAALOUNI YATHREB ABDELLAOUI*
LAKDAR KAIROUANI KAIROUANI

National Engineering School of Tunis ENIT, BP 37 1002 Runis, Tunisia

Abstract In this work, a new dual-evaporator CO_2 transcritical refrigeration cycle with two ejectors is proposed. In this new system, we proposed to recover the lost energy of condensation coming off the gas cooler and operate the refrigeration cycle ejector free and enhance the system performance and obtain dual-temperature refrigeration simultaneously. The effects of some key parameters on the thermodynamic performance of the modified cycle are theoretically investigated based on energetic and exergetic analysis. The simulation results for the modified cycle indicate more effective system performance improvement than the single ejector in the CO_2 vapor compression cycle using ejector as an expander ranging up to 46%. The exergetic analysis for this system is made. The performance characteristics of the proposed cycle show its promise in dual-evaporator refrigeration system.

Keywords: CO_2; Energy; Refrigeration; Ejector; Exergy

Nomenclature

A	–	section, m^2
COP	–	coefficient of performance
h	–	specific enthalpy, kJ kg^{-1}
I	–	irreversibility, kJ kg^{-1}
$\dot{m}$	–	mass flow rate, kJ kg^{-1}

*Corresponding Author. E-mail: ezzaalouni.yathreb26@gmail.com

P	–	pressure, MPa
Q_e	–	cooling capacity rate, kW
S	–	specific entropy, $\mathrm{kJ\,kg^{-1}K^{-1}}$)
T_0	–	environmental temperature, K
T_r	–	the temperature of secondary fluid in the evaporator, K
V	–	velocity, $\mathrm{ms^{-1}}$
U	–	entrainment ratio
W	–	mechanical power rate, kW

Greek symbols

ε	–	error
η	–	efficiency, %
ξ	–	driving pressure ratio, P_3/P_6
ρ	–	pressure lift ratio, P_6/P_1

Subcripts and superscripts

1,2,3,...,13	–	thermodynamic states of fluid in the refrigeration cycles
0	–	state of reference
a	–	schematic system
b	–	p-h diagram
c	–	compressor
$cond$	–	condenser
d	–	diffuser
e	–	evaporator
ej	–	ejector
ev	–	expansion valve
i	–	intermediate state
in	–	inlet
is	–	isentropic process
gc	–	gas cooler
gen	–	generated
k	–	summation index
m	–	mixing section
n	–	nozzle suction
out	–	outlet
p	–	pump
tot	–	total
opt	–	optimal
$'$	–	primary fluid (or motive fluid)
$''$	–	secondary fluid (or entrained aspirated)

1 Introduction

Nowadays, a large proportion of industrial areas use extensively compressed refrigeration cycle, which consumes a considerable share of social energy [1]. The critical influence of the refrigeration industry on global warming and the allocation of the ozone layer has become a challenge that is the subject of several researches. The appropriate choice of cycle configuration and of environmentally friendly refrigerants for these refrigeration systems has a positive effect on energy savings and lower greenhouse gas emissions. The natural working fluid such as CO_2 can be a promoter alternative refrigerant to replace chlorofluorocarbons (CFCs) and hydrochlorofluorocarbons (HCFCs) because of its friendly environmental characteristics and excellent heat transfer.

But, the refrigeration system using CO_2 has an operating stress that it must be operated with a transcritical cycle mode because of the lower critical temperature of CO_2, and their coefficient of performance (COP) is lower than that of conventional cycle using CFCs and HCFCs refrigerants due to oversized expansion losses [2]. Therefore, a large amount of efforts such as employing additional ejector [3–5] or the expander [6–9] have been made by researchers to recover the throttling losses in the systems. In recent years, ejectors have been getting more attention due to their noticeable features, such as low cost, no moving parts, low maintenance requirements, simple structure, and high performance improvement potential. Therefore, lots of experimental and theoretical literatures about ejector enhanced transcritical CO_2 heat pump and refrigeration cycle have been made recently. The research results show that use of ejector as an expander in transcritical CO_2 cycle is considered to be a promising cycle modification to improve the system performance [10–15].

As well known, multitemperature refrigeration systems have gained greater popularity due to their potential applications in a wide range of cooling temperatures. Besides widely used refrigerator-freezer for households, the two-stage compression CO_2 refrigeration cycle with different temperatures also has been getting a growing concern. Sharma *et al.* [16] presented an optimizing analysis on the various multitemperature transcritical cycles including cascaded and secondary loop refrigeration cycle systems which are becoming popular in the supermarket applications.

Shin *et al.* [17] modeled the two-stage compression CO_2 refrigeration cycle with two different evaporating temperatures by taking into account the frost growth condition and investigated effects of frost growth on the system performances. Generally, in a multitemperature refrigeration system large thermodynamic losses in throttling processes can be generated if conventional expansion devices are used. From an exergetic viewpoint, nonetheless, the system performance again, has a large potential sophistication. An effective method of improving the system performance is to recover the expansion work in the throttling processes. During the past years, various cycle design employing ejector have been developed for the energy saving purpose [18–24]. The specialized literatures generally are concentrated on the single ejector enhanced multievaporator refrigeration cycles to recover the expansion losses.

Kairouani *et al.* [19] theoretically analyzed a three cooling temperatures refrigeration cycle with two stage ejector, and made clear that the two-stage ejector are efficient to recover pressure losses in the multi-evaporator refrigeration system. Lin *et al.* [20–22] experimentally estimated the performance of three-circuit refrigeration configuration with the adjustable ejectors. Zhou *et al.* [23] presented a two-circuit refrigeration cycle with a novel dual-nozzle ejector and found the COP could be improved by 22.9–50.8%.

Hafner *et al.* [24] theoretically investigated efficiency and capacity of the CO_2 supermarket layouts with multiejector and heat recovery under different climate conditions and the achieved system efficiency improvement could be up to 30%. Based on the literatures introduced above, we can see that small care has been paid to the CO_2 transcritical dual evaporator refrigeration cycle.

In this paper, we propose a new cycle. The major advantage of this cycle configuration is the ability to sufficiently recover the condensation energy to operate the second cycle and to ensure the dual-temperature refrigeration function. For thermodynamic performances of the proposed cycle, energetic and exergetic methods are applied in this paper, and the performance of the novel cycle is compared to the conventional cycle.

2 Cycle system description

The schematic of a conventional vapor compression refrigeration cycle using ejector as an expander is shown in Fig. 1. This system includes a compressor, a gas cooler, an expansion valve, separator, ejector and evaporator. The thermodynamic processes of conventional vapor compression cycle represent the compression, heat rejection, expansion and evaporation. It is recognized that the isenthalpic expansion processes in this cycle leads to lower system performance due to the higher irreversibility of the expansion valves. So, it should be noted, that the use of an ejector as the expansion device improves the thermodynamic performance this system, because ejec-

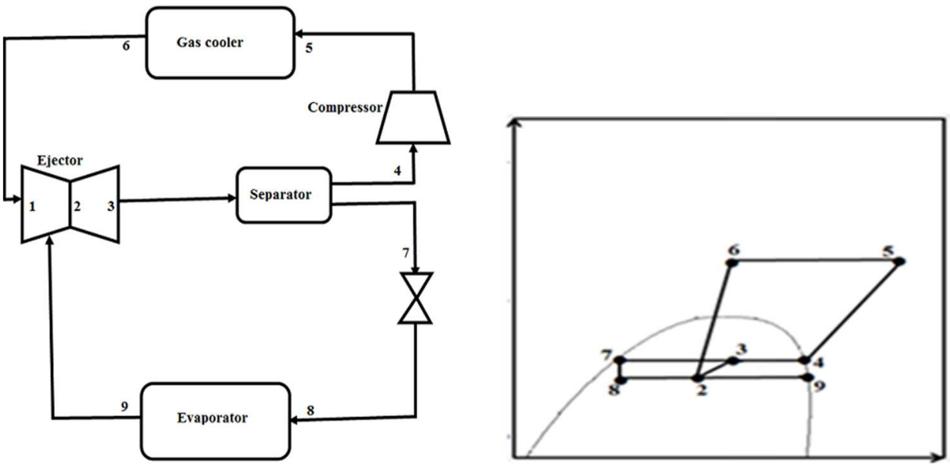

(a) (b)

Figure 1: (a) Schematic of vapor compression cycle using ejector as an expander, (b) pressure-enthalpy diagram.

tor can effectively recover the expansion work to lift the suction pressure and enhance the system performance. Without a doubt, a suitable ejector configuration with a better pressure lifting performance must be desired.

Figure 2 shows a schematic and the corresponding pressure-enthalpy diagram of a novel refrigeration cycle with two ejectors. The high temperature CO_2 enters the compressor at pressure P_4 at state (4) in which it is compressed to the pressure P_5, with an isentropic efficiency, η_c thereafter the compressed fluid at state (5) is cooled in the gas cooler to the temperature T_6. The CO_2 at state (6) enters the ejector nozzle and expands with a nozzle efficiency of η_n. The saturated secondary vapor stream enters the ejector at pressure P_9 in accordance with the state (9). The two streams mix at constant pressure in the final state of the mixture according to state (3). It is necessary to know that after that the mixture goes through the ejector diffuser with a diffuser efficiency of η_d, in which recovers to the pressure P_3 at state (3), the stream leaves the ejector and then flows into the separator, where it is separated to two distinct states; saturated liquid and saturated vapor, while the saturated liquid stream enters the conventional expansion valve and expands to pressure P_{eva} at state (8), the saturated vapor enters to the compressor at state (4).

The ejector refrigeration cycle is a one phase expanding process. It presents rather low performance. The cycle is generally used with the waste

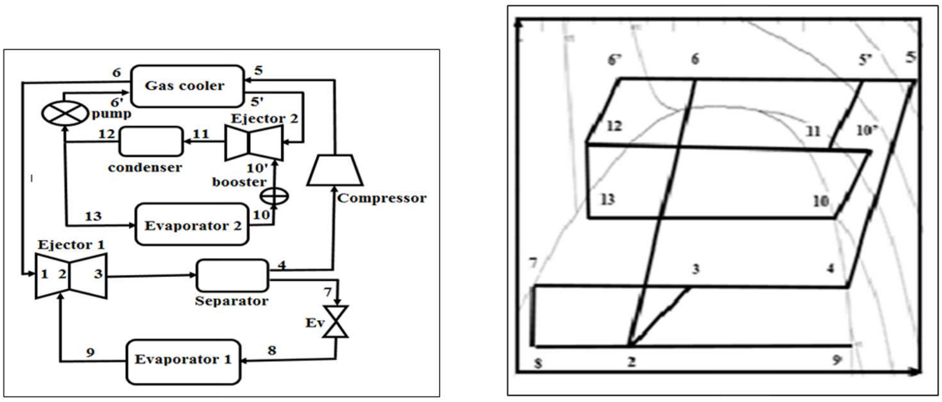

(a) (b)

Figure 2: (a) Schematic of a novel refrigeration cycle with two ejectors, (b) pressure-enthalpy diagram.

heat or solar energy as boiler heat source to enhance the performances. For this reason it is proposed to operate the system for free by recovering the amount of condensation heat.

The liquid flow exiting the condenser is divided into two parts: one flow is expanded into the evaporator, and the other is compressed by a liquid pump to a high pressure. The high pressure flow enters the gas cooler where it will be vaporized and heated. The superheated high-pressure vapor enters the booster in which it undergoes a slight increase in pressure and leaves towards the ejector nozzle. Next it expands in the nozzle to vapor flow at a low pressure able to absorb vapor from the evaporator, then the two vapor flows are mixed in the mixture chamber before entering the diffuser that will decelerate the mixture velocity. After, the vapor ejector outlet flow enters the condenser.

3 Performance analysis

3.1 Analysis of the ejector

The ejector under consideration is shown in Fig. 3. The motive flow coming from the gas cooler enters the ejector at a relatively high pressure and zero velocity, i.e., stagnation condition corresponding to state (0) and expands to a pressure at state (1). The secondary flow from the evaporator is then induced into the ejector by the low pressure flow at its nozzle exit. Both fluids mix together in the mixing chamber section. The mixed flow at the end of the mixing duct state (2) is discharged into a diffuser, and then the diffused flow exits from the ejector at section (3) to the separator. To simplify this analysis, the following assumptions are made in this study:

1. The refrigerant was at all times in thermodynamic quasiequilibrium.
2. Characteristics and velocities were constant over the cross section (one-dimensional model).
3. All fluid characteristics are uniform over the cross section after complete mixing at the exit of the mixing tube.
4. There is no external heat transfer.
5. There is no wall friction.

The control volume between sections 1 and 3 is divided into two regions and those are the control volume 1–2 and 2–3 as shown in Fig. 3.

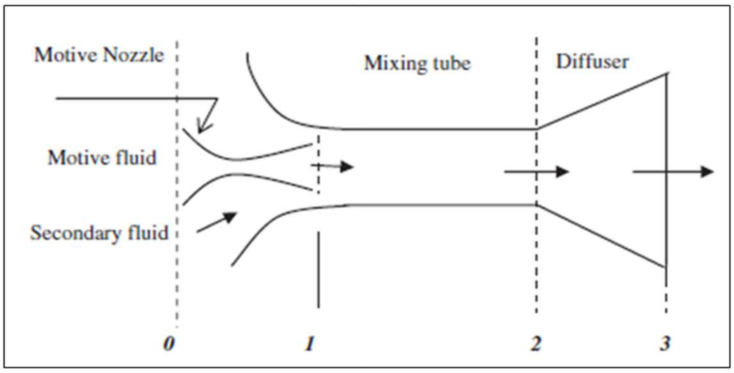

Figure 3: Configuration of the ejector.

3.1.1 Flow nozzle

The exit velocity from the nozzle is calculated from

$$V_1 = \sqrt{2\eta\ (h_e - h_1)}\ , \tag{1}$$

where h_1 is the enthalpy at the outlet of the motive nozzle for an isentropic process

$$h_1 = h\ (S_e,\ P_1\ )\ , \tag{2}$$

$$h_{1a} = h_1 - \eta (h_e - h_1) \ . \tag{3}$$

The density, at the outlet of the motive nozzle, is calculated from h_{1a} and P_1 as

$$\rho_1 = \rho\ (h_{1a},\, P_1)\ . \tag{4}$$

The mass flow rate is

$$\dot{m}' = \rho_1 V_1\ A_1\ . \tag{5}$$

3.1.2 Flow in the mixing chamber

Using the continuity equation, the total mass flow through the mixing tube is computed as

$$\dot{m}' + \dot{m}'' = \rho_2 A_2 V_2\ . \tag{6}$$

The momentum balance of the mixing tube yields

$$(P_2 - P_1)\, A_2 = \dot{m}' V_1 - (\dot{m}' + \dot{m}'') V_2\ . \tag{7}$$

Combining Eqs. (6) and (7) we can obtain the pressure rise in the mixing tube from

$$\frac{P_2 - P_1}{\frac{1}{2}\rho_1 V_1^2} = 2\frac{A_1}{A_2} - 2(1+U)^2 \frac{\rho_1}{\rho_2}\left(\frac{A_1}{A_2}\right)^2\ , \tag{8}$$

where $U = \dot{m}''/\dot{m}'$ represents the flow entrainement ratio and the density ratio, ρ_1/ρ_2 can be approximated as [25]

$$\frac{\rho_2}{\rho_1} = \frac{U}{1+U}\frac{\rho_v}{\rho_1} + \frac{1}{1+U}\ , \tag{9}$$

where ρ_v is the refrigerant's vapour density at the evaporator outlet.

The mixing velocity is defined as

$$V_2 = \frac{1}{1+U} V_1\ . \tag{10}$$

The velocity at the outlet section nozzle is insignificant.

At the outlet of the mixing section, by conservation of energy

$$h_2 = \frac{1}{1+U} h_c + \frac{U}{1+U} h_e - \frac{V_2^2}{2}\ . \tag{11}$$

The entropy, at the outlet of the mixing section, is calculated from h_2 and P_2

$$S_2 = S_2(h_2, P_2)\ . \tag{12}$$

3.1.3 Diffuser flow

At the outlet of the diffuser, by conservation of energy

$$h_3{=}h_2{+}V_2^2\ . \tag{13}$$

The exit diffuser velocity is insignificant, so the exit diffuser enthalpy can be written as

$$h_{3a}{=}h_2{+}\eta_d\frac{V_2^2}{2}\ . \tag{14}$$

The exit diffuser pressure is defined by S_2 and h_{3a}

$$P_3{=}\ P(S_2, h_{3a})\ . \tag{15}$$

From P_3 and h_3, the exit diffuser intensive state is known (x_3, r_3 ...).

When the geometry parameters of the ejector are known, such as A_2/A_1; the efficiencies of nozzle and diffuser and the operating conditions, we can determine the outlet diffuser parameters such as P_3 and h_3.

3.2 Mass analysis

We must verify that the mass conservation equation is satisfied for each element of the system as is mentioned below

$$\sum m_{in} = \sum m_{out}\ .$$

3.3 Energy analysis

Modeling of the system has taken into account the following assumptions:

(1) compression process within compressor is completely adiabatic,

(2) pressure drops in pipelines, and heat exchanger is neglected,

(3) throttling process within expansion valve is at constant enthalpy,

(4) mixing pressure in the ejector is equal to the evaporator pressure,

(5) outlet states of the condenser and the middle condenser are at saturated liquid states and the evaporator 1 and 2 are at saturated vapor state,

(6) pumping process is isentropic,

(7) modeling of the ejector 1 follows the model of constant pressure [26] against the second follows the model of constant section [27],

(8) ambient temperature, 25 °C.

3.4 Energy analysis for conventional refrigeration system using ejector as an expander

For the compressor, its power consumption is

$$W_c = \frac{1}{1+U}(h_5 - h_4)\ . \tag{16}$$

The compressor's adiabatic efficiency is [26]

$$\eta_c = 0.874 - 0.0135(P_5/P_4)\ . \tag{17}$$

For the gas cooler the heat transfer rate of the gas cooler is

$$Q_{gc} = \frac{1}{1+U}(h_6 - h_5)\ . \tag{18}$$

For the expansion valve, it is assumed that the relaxation process is isenthalpic

$$h_7 = h_8\ . \tag{19}$$

For the evaporator, the cooling capacity is

$$Q_e = \frac{U}{1+U}(h_9 - h_8)\ . \tag{20}$$

For the ejector

$$h_3 = \frac{1}{1+U}(h_6 - Uh_9)\ . \tag{21}$$

The system's performance is evaluated by the coefficient of performance (COP), which is the ratio of the cooling capacity to the power absorbed by compressor

$$COP = \frac{Q_e}{W_c}\ . \tag{22}$$

3.4.1 Energy analysis for new refrigeration system

For the compressor, his power consumption is:

$$W_c = \frac{1}{1+U}(h_5 - h_4)\ . \tag{23}$$

For the gas cooler: the heat transfer rate of the gas cooler is

$$\dot{m}'\ (h_{6'} - h_{5'}) = \frac{1}{1+U}(h_6 - h_5)\ . \tag{24}$$

For the expansion valve, it is assumed that the relaxation process is isenthalpic

$$h_7 = h_8 \; . \tag{25}$$

For the evaporator 1, the cooling capacity is

$$Q_{e1} = \frac{U}{1+U}(h_9 - h_8) \; . \tag{26}$$

For the ejector 1

$$h_3 = \frac{1}{1+U}(h_6 - Uh_9) \; . \tag{27}$$

For the pump

$$W_p = \dot{m}^{'} \; (h_{6'} \; - h_{12}) \; . \tag{28}$$

For expansion valve 2

$$h_{12} \; = h_{13} \; . \tag{29}$$

For condenser

$$Q_{cd} = (\dot{m}^{'} + \dot{m}^{''})(h_{12} - h_{11}) \; . \tag{30}$$

For evaporator 2

$$Q_{e2} = \dot{m}^{''}(h_{13} - h_{10}) \tag{31}$$

For booster

$$W_b = \dot{m}''(h_{10'} - h_{10}) \; . \tag{32}$$

For ejector 2

$$(\dot{m}^{'} + \dot{m}^{''})h_{11} = \dot{m}^{'}h_{5'} + \dot{m}^{''}h_{10'} \; . \tag{33}$$

The system's performance is evaluated by the coefficient of performance COP, which is the ratio of the cooling capacity to the power absorbed by compressor

$$COP_{new\ cycle} = \frac{Q_{e1} + Q_{e2}}{W_c + W_p + W_b} \; . \tag{34}$$

3.5 Exergy analysis

According to [27], entropy generation rate for a fixed control volume is presented through the following relation:

$$\dot{S_{gen}} = \sum \dot{m}_0 S_0 - \sum \dot{m}_i S_i - \sum \frac{Q_k}{T_k} \; . \tag{35}$$

When the kinetic and potential energies are neglected, according to [30], the physical exergy can be measured by

$$\Psi = (h - h_0\ ) - T_0(S{-}S_0)\ . \tag{36}$$

The exergy destruction rate can also be defined by applying the Gouy-Stodola theorem as below

$$I = T_0\dot{S}_{gen}\ . \tag{37}$$

For each individual component, the equation of the exergy destruction rate based on specific mixture mass flow rate can be written as following

3.5.1 Exergy analysis for conventional refrigeration system using ejector as an expander

For the compressor

$$I_c = \frac{1}{1+U}\ T_0(S_5\ -\ S_4)\quad . \tag{38}$$

For the gas cooler

$$I_{gc} = \frac{1}{1+U}\ (h_2\ -\ h_3\ -\ T_0(S_6\ -\ S_5)) \tag{39}$$

For the expansion valve

$$I_{ev} = \frac{U}{1+U}\ T_0\ (\ S_8\ -\ S_7\ ) \tag{40}$$

For the evaporator

$$I_e = \frac{U}{1+U}\ \ T_0\left[\ (\ S_9\ -\ S_8\ )\ -\ \frac{h_9\ -\ h_8}{T_r}\right]\quad . \tag{41}$$

For the ejector

$$I_{ej} = T_0\left[\ S_3\ -\ \frac{(\ S_6\ +U\ S_9)}{(\ 1+\ U\ )}\right]\ . \tag{42}$$

3.5.2 Exergy analysis for new refrigeration system

For the compressor

$$I_c = \frac{1}{1+U}\ T_0\ \ (S_5{-}\ S_4)\ . \tag{43}$$

For the gas cooler

$$I_{gc} = T_0 \left[\frac{(S_6 - S_5)}{(1+U)} + \dot{m}' \ (S_{6'} - S_{5'}) \right] . \tag{44}$$

For the expansion valve 1

$$I_{ev1} = \frac{U}{1 \ + \ U} \ T_0 \, (s_7 - s_6) \ . \tag{45}$$

For the evaporator 1

$$I_{e1} = \frac{U}{1+U} \ T_0 \left[(S_9 - S_8) - \frac{(h_8 - h_7)}{T_{r1}} \right] . \tag{46}$$

For the ejector 1

$$I_{ej1} = T_0 \ \left[S_3 - \frac{(S_6 + U \ S_9)}{(1+U)} \right] . \tag{47}$$

For the pump

$$I_p = \dot{m}' \ T_0 \, (S_{6'} - S_{12}) \ . \tag{48}$$

For the expansion valve 2

$$I_{ev2} = \dot{m}'' \ T_0 \, (S_{13} - S_{12}) \ . \tag{49}$$

For the condenser

$$I_{cond} = \left(\dot{m}' + \dot{m}'' \right) \left[\, (h_{12} - h_{11}) - T_0 \ \ (S_{12} - S_{11}) \, \right] . \tag{50}$$

For the evaporator 2

$$I_{e2} = \dot{m}'' T_0 \left[(S_{10} - S_{13}) - \frac{(h_{10} - h_{13})}{T_{r2}} \right] . \tag{51}$$

For the booster

$$I_b = \dot{m}'' T_0 \left(S_{10'} - S_{10} \right) \ . \tag{52}$$

For the ejector 2

$$I_{ej2} = T_0 \left[\left(\dot{m}' + \dot{m}'' \right) S_{11} - \left(\dot{m}' S_{10} + \dot{m}'' S_{5'} \right) \right] . \tag{53}$$

The total exergy destruction rate of the cycle is the sum of the exergy destruction rate in each component

$$I_{tot} = I_c \ + I_{gc} + I_{ev1} + \ I_{e1} + \ I_{ej1} + I_p + I_{ev2} + \ I_{e2} + \ I_{cd} + \ I_b + I_{ej2} \ . \tag{54}$$

The overall exergy efficiency of the new system can be evaluated by the ratio of the effective exergy output to the rate of exergy input, and the effective exergy output can be gained by subtracting the total exergy destruction from the effective exergy input. Thus the exergetic (second law) efficiency of the system can be given as

$$\eta_{II}= 1-\frac{I_{tot}}{W_c+W_p + W_b} \ . \tag{55}$$

4 Result and discussion

To inquire the performances characteristic of the modified cycle, the simulation conditions are given as follows: the gas cooler exit temperature, T_{gc}, ranges from 35 to 50 °C, the evaporating temperature, T_{e1}, ranges from -50 to -35 °C, the evaporating temperature T_{e2} ranges from -20 to -10 °C, the condensing temperature, T_{cond}, ranges from 18 to 25 °C , the temperature difference between refrigerant and cooled space is taken as a constant, $\Delta T = 5\,°\mathrm{C}$, the gas cooler pressure, P_{gc}, varies from 8.5 to 11.5 MPa. For simplicity, the ejector efficiencies are assumed $\eta_n = \eta_d = 0.85$.

In the following analysis, effects of discharge pressure, evaporating temperature, gas cooler exit temperature and the refrigeration capacity ratio on the system performances are studied, respectively.

4.1 Ejector model validation

Ejector is the critical component in the ejector enhanced refrigeration cycles and its performance is closely related to the system performance and energy efficiency. Therefore, establishing a valid simulation model plays a significant role in the prediction and analysis of the operating characteristics of the ejector enhanced system.

In order to validate the simulation models, the available data in literature were used. The operating and design parameters are assumed to be exactly the same as those in the literature. The thermodynamic model of the ejector was validated using the previously published experimental data (Elias Bou Lawz Ksayer [31]: using R744 as refrigerant, and Huang *et al.* [32]: using R141b as working fluid) and the results of comparison is shown in Tabs. 1 and 2.

The results of validation shown in Tabs. 1 and 2 indicate a good agreement between the present results and those published in the literature. The comparison of calculated error confirms that the present model could accurately predict the experimental model with the maximum deviation is 6.85% and 7.45%, respectively.

Table 1: Comparisons of test and analytical results COP systems; error ε = (theory – experiment)/experiment).

T_e (°C)	T_{gc} (°C)	$COP_{present\,study}$	COP_{exp} [29]	ε (%)
-1	32	4.02	3.82	5.23
-1	34	3.78	3.5	6.57
-1	36	3.10	3.2	-3.12
2	32	4.43	4.2	5.47
2	34	4.08	4.0	2.00
2	36	3.74	3.5	6.85

Table 2: Comparisons of test and analytical results ejector specification; error ε = (present study – experiment)/experiment).

T_c	$U_{present\,study}$	$U_{experimental}$ [30]	ε (%)
31.3	0.448	0.4377	2.34
33.6	0.3715	0.3457	7.45
28.0	0.525	0.5387	-2.54
30.5	0.412	0.4241	-2.86
33.1	0.521	0.4989	4.42
34.5	0.436	0.4541	-3.98
28.9	0.605	0.6350	-4.71
32.4	0.452	0.4790	-5.42

4.2 Impact of gas cooler pressure

Figure 4 shows the effects of gas cooler pressure, P_{gc}, on the COP, and $COP_{new\,syst}$. It can be observed that there exists an optimum pressure around 9 MPa where the both system COP and $COP_{new\,cycle}$ reach the maximum values at the given operating condition. When the gas cooler pressure varies from 8 to 11 MPa, the COP, and $COP_{new\,syst}$ in the ranges of 1.1–1.23 and 1.46–1.76, respectively. For the same operating conditions and at the optimum gas cooler pressure, it confirms the improvement of COP ranging up to 44% and puts in evidence our contribution to improve cycle performance in question.

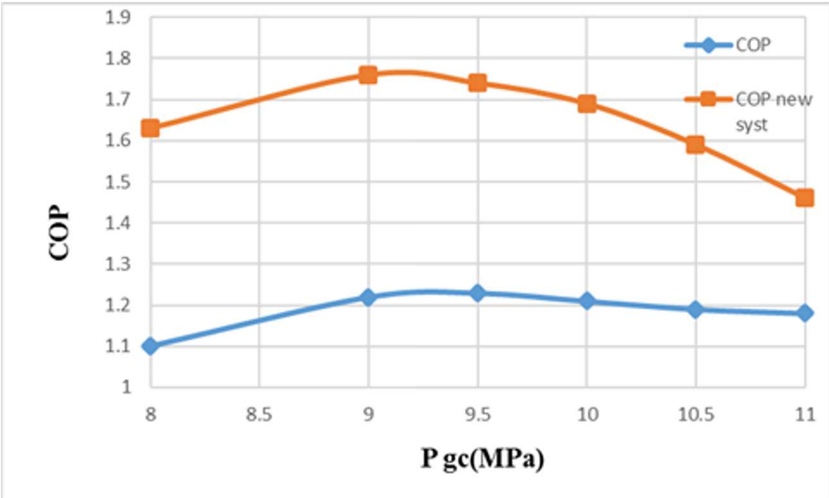

Figure 4: Comparing the performance system with P_{gc} ($T_{gc} = 35\,°\mathrm{C}$, $T_{e1} = -50\,°\mathrm{C}$, $Te_2 = -20\,°\mathrm{C}$, $T_{cond} = 25\,°\mathrm{C}$).

Figure 5 shows the effects of gas cooler temperature, T_{gc}, on the $COP_{new\,syst}$; it can be seen that $COP_{new\,syst}$ decreases with the increasing gas cooler exit temperature for different values of P_{gc}. Figures 6 and 7 show respectively the effect of P_{gc} and T_{gc} on the second law efficiency, η_{II}, and I_{tot}. It indicates that the total exergy destruction rate increases as the gas cooler outlet temperature increases. It is due to higher irreversibility rates at high gas cooler outlet temperatures.

The new refrigeration cycle has a reduced value of the total irreversibility, because the irreversibility in the gas cooler is drastically less than that of the conventional cycle. It is remarkable that the gas cooler temperature, T$_{gc}$, and pressure, P_{gc}, influences the total irreversibility. It decreases as the gas cooler temperature increases. Also, the I_{tot} decreases as the gas cooler temperature increases.

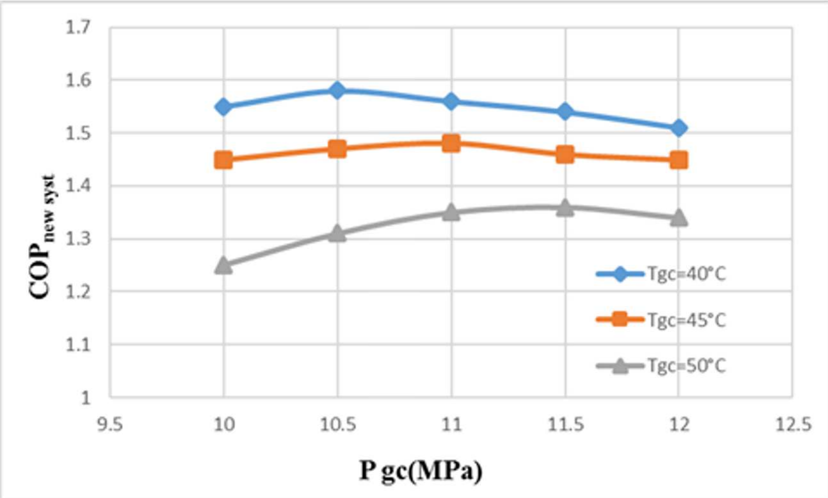

Figure 5: Effect of T_{gc} on COP ($T_{cond} = 25\,^\circ$C, $T_{e1} = -50\,^\circ$C, $T_{e2} = -20\,^\circ$C).

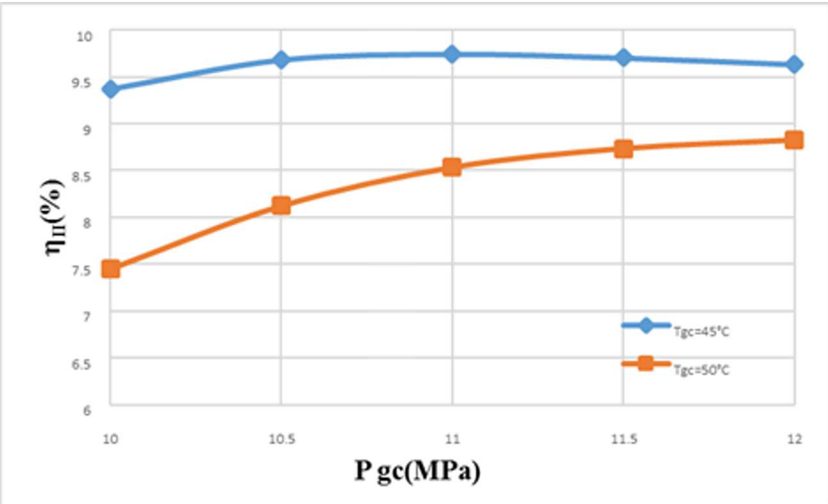

Figure 6: Effect of P_{gc} and T_{gc} on the second law efficiency $\eta_{II}(\%)$($T_{cond} = 25\,^\circ$C, $T_{e1} = -50\,^\circ$C, $T_{e2} = -20\,^\circ$C).

4.3 Impact of condensing temperature

Figure 8 shows that the coefficient of performance increase with decreasing of condensing temperature, T_{cond}, and attest that for any value of T_{cond} there is a P_{gc} value for what the $COP_{new\,syst}$ reaches its optimum, for

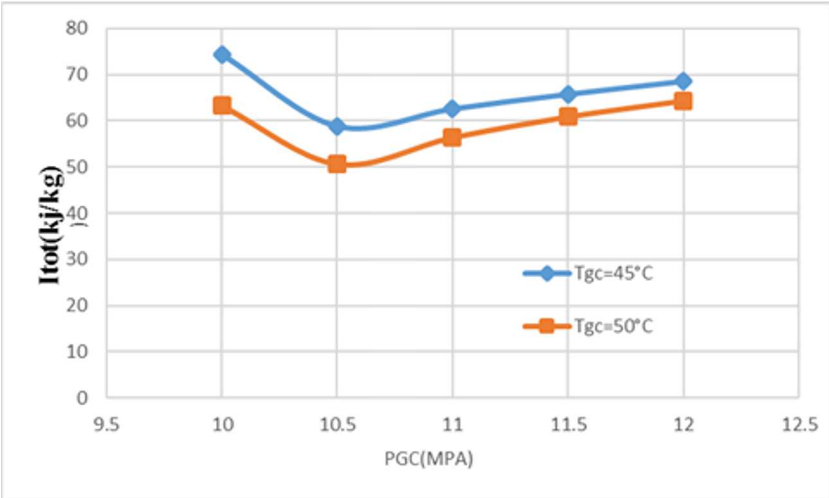

Figure 7: Effect of P_{gc} and T_{gc} on I_{tot} ($T_{cond} = 25\,^{\circ}$C, $Te_1 = -50\,^{\circ}$C, $T_{e2} = -20\,^{\circ}$C).

example for $T_{cond} = 25\,^{\circ}$C, the $COP_{new\,syst}$ reaches maximum value 1.6 for $P_{gc,opt} = 9.5$ MPa.

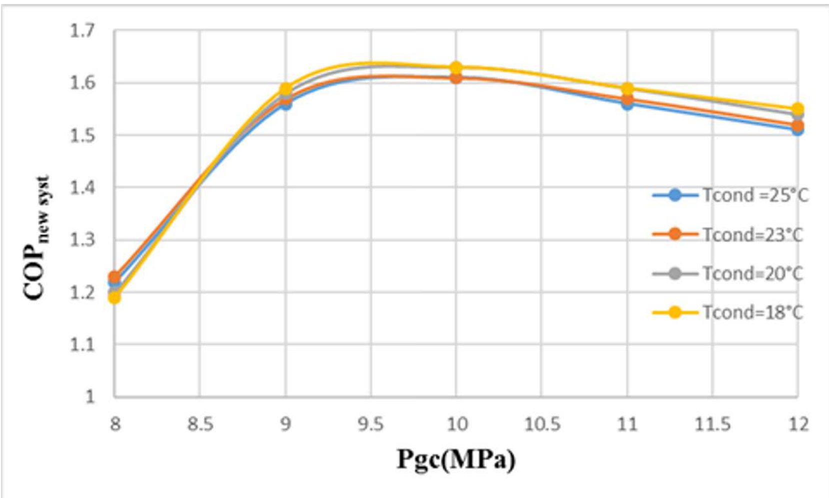

Figure 8: Variation of COP with T_{cond} ($T_{e1} = -50\,^{\circ}$C, $T_{e2} = -20\,^{\circ}$C, $T_{gc} = 40\,^{\circ}$C).

Figures 9 and 10 show the influence of T_{cond} on the irreversibility, we see that increasing of T_{cond} induces decreased irreversibility of the system

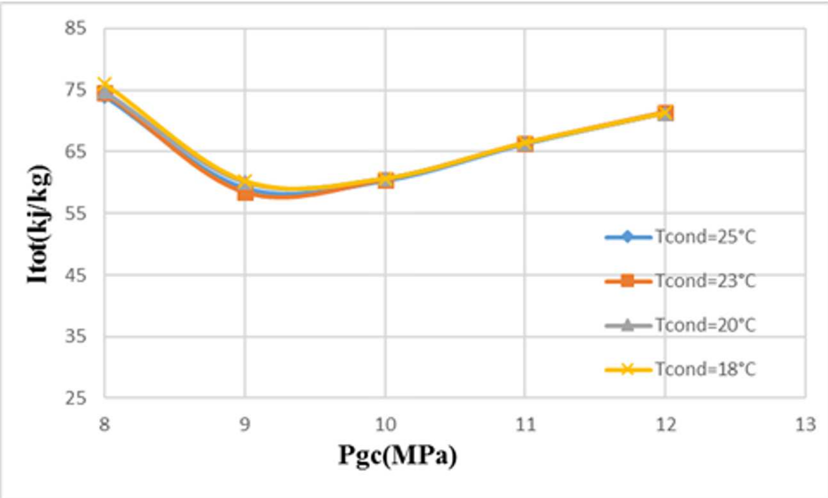

Figure 9: Effect of T_{cond} on the total irreversibility I_{tot} (T_{gc} = 40 °C, T_{e1} = −50 °C, T_{e2} = −20 °C).

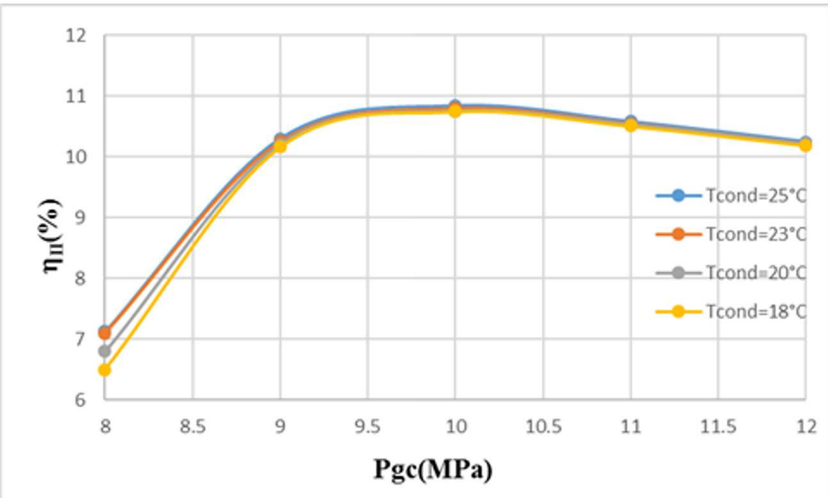

Figure 10: Effect of T_{cond} on the second law efficiency (T_{gc} = 40 °C, T_{e1} = −50 °C, T_{e2} = −20°C).

which explains the rating increase of the second law efficiency throughout the Fig. 10.

4.4 Impact of evaporator temperature

Figure 11 shows the influence of T_{e1} on the coefficient of performance. We see that increasing of T_{ev1} induces increased performances of the new system. Figure 12 depicts the variation of the total exergy destruction rate of the new cycle versus the evaporating T_{e1}. As the evaporating temperature increases, the exergy destruction rate of the system decreases.

The variation of the second law efficiency with the evaporating temperature T_{e1} is shown in Fig. 13. It can be seen that the second law efficiency increases as the evaporating temperatures decrease. It can be accounted as an advantage of the new cycle in applications with lower refrigeration temperature.

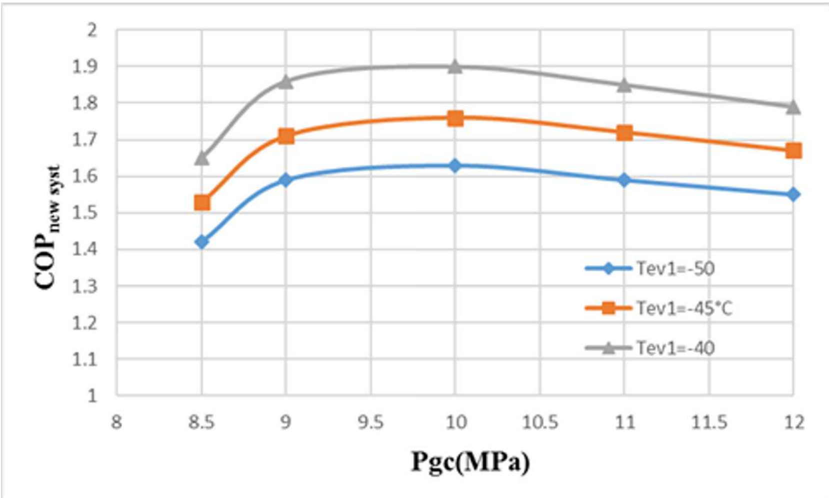

Figure 11: Effect of T_{e1} on $COP_{new\,syt}$ ($T_{gc} = 40\,^{\circ}$C, $T_{e2} = -20\,^{\circ}$C, $T_{cond} = 18\,^{\circ}$C).

5 Conclusion

A combined dual-evaporator transcritical CO_2 refrigeration system is proposed in this paper. Energetic and exergetic analysis are conducted to evaluate thermodynamic performances of this cycle. The effects of key operating parametric on performance are discussed. From the discussion above, the modified cycle could simultaneously obtain dual cooling temperatures with higher COP and exergy efficiency.

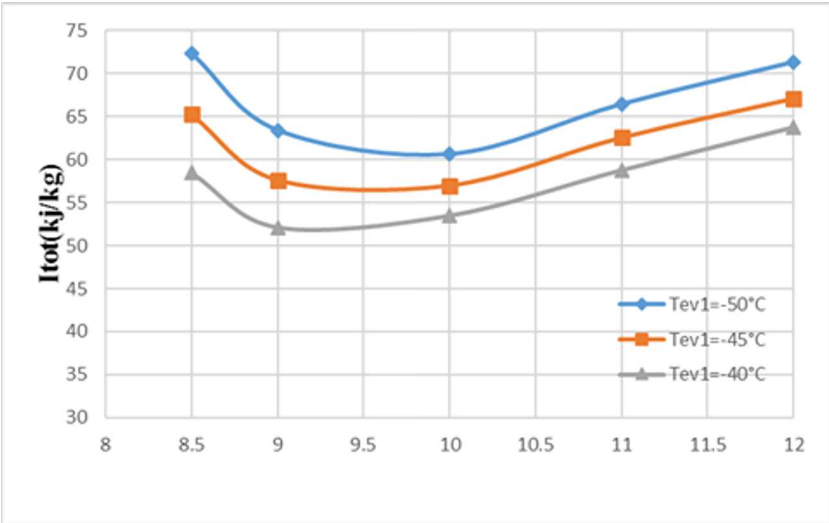

Figure 12: Effect of T_{e1} on I_{tot} ($T_{cond} = 18\,^{\circ}$C, $T_{e2} = -20\,^{\circ}$C, $T_{gc} = 40\,^{\circ}$C).

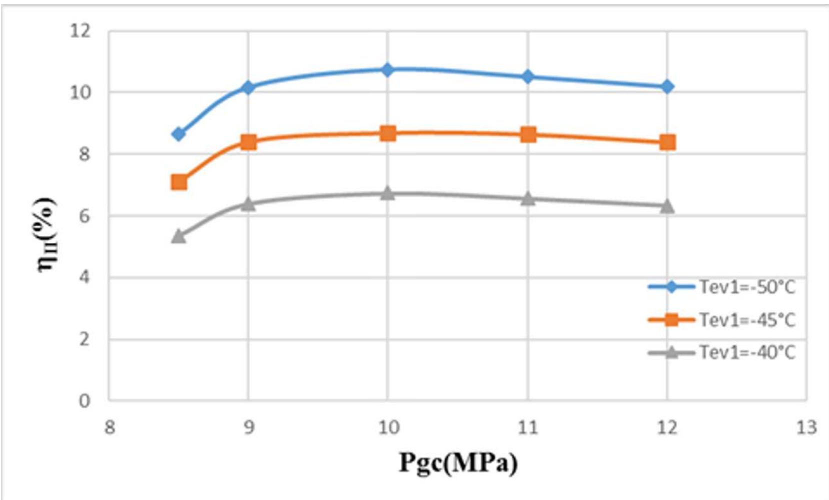

Figure 13: Effect of T_{e1} on the second law efficiency ($T_{gc} = 40\,^{\circ}$C, $T_{e2} = -20\,^{\circ}$C, $T_{cond} = 18\,^{\circ}$C).

Meanwhile this cycle presents an opportunity to recover the lost energy of condensation coming off the gas cooler and operate the refrigeration cycle ejector free. The parametric study shows that discharge pressure, evaporating temperature and gas cooler exit temperature have significant effects on system COP and exergy efficiency. It should be mentioned that although the computational model developed for the ejector is relatively simple in respect of its practical application in real system, it is hoped that the proposed cycle could provide useful guidance to the development of dual-evaporator transcritical CO_2 refrigeration. Thus, it should be emphasized that further studies, especially experimental studies, are needed to confirm the practical usefulness of this cycle.

Received 17 February 2017

References

[1] Radermacher R., Kim K.: *Domestic refrigerators: recent developments*. Int. J. Refrig. **19**(1996), 1, 61–69.

[2] Liu F., Groll E.A.: *Study of ejector efficiencies in refrigeration cycles*. Appl. Therm. Eng. **52**(2013), 2, 360–370.

[3] Chunnanond K., Aphornratana S.: *Ejectors: applications in refrigeration technology*. Renew. Sust. Energ. Rev. **8**(2004), 2, 129–155.

[4] Chen X., Omer S., Worall M., Riffat S.: *Recent developments in ejector refrigeration technologies*. Renew. Sust. Energ. Rev. **19**(2013), 629–651.

[5] Groll E.A., Kim J-H.: *Review article: review of recent advances toward transcritical CO2 cycle technology*. HVAC&R Res **13**(2007), 3, 499–520.

[6] Lu Y., He W., Wu Y., Ji W., Ma C., Guo H.: *Performance study on compressed air refrigeration system based on single screw expander*. Energy **55**(2013), 762-768.

[7] Yang J.L., Ma Y.T., Liu S.C.: *Performance investigation of transcritical carbon dioxide two-stage compression cycle with expander*. Energy **32**(2007), 3, 237–245.

[8] Kozioł J., Gazda W., Wilżyński Ł.: *Energy efficiency for the transcritical compression CO2 cycle with the use of the ejector as the first stage of the compression*. Arch. Thermodyn. **31**(2010), 4, 61–69.

[9] Dudar A., Butrymowicz D., Śmierciew K., Karwacki J.: *Exergy analysis of operation of two-phase ejector in compression refrigeration systems*. Arch. Thermodyn. **34**(2013), 4, 107–122.

[10] Liu J.P., Chen J.P., Chen Z.J.: *Thermodynamic analysis on trans-critical R744 vapor compression/ejection hybrid refrigeration cycle*. In: Proc. Fifth IIR-GUSTAV Lorentzen Conference on Natural Working Fluids, Guangzhou 2002.

[11] Yari M., Sirousazar M.: *Cycle improvements to ejector-expansion transcritical CO_2 two-stage refrigeration cycle*. Int. J. Energy Res. **32**(2008), 7, 677–687.

[12] Sun F.T., Ma Y.T.: *Thermodynamic analysis of transcritical CO2 refrigeration cycle with an ejector*. Appl. Therm. Eng. **31**(2011), 6-7, 1184–1189.

[13] Elbel S., Hrnjak P.: *Experimental validation of a prototype ejector designed to reduce throttling losses encountered in transcritical R744 system operation*. Int. J. Refrig. **31**(2008), 3, 411–422.

[14] Manjili F.E, Yavari M.A.: *Performance of a new two-stage multi-intercooling transcritical CO2 ejector refrigeration cycle.* Appl. Therm. Eng. **40**(2012), 202–209.

[15] Li D.Q., Groll E.A.: *Transcritical CO2 refrigeration cycle with ejector-expansion device.* Int. J. Refrig. **28**(2005), 5, 766–773.

[16] Sharma V., Fricke B., Bansal P.: *Comparative analysis of various CO_2 configurations in supermarket refrigeration systems.* Int. J. Refrig. **46**(2014), 86–99.

[17] Shin E., Park C., Cho H.: *Theoretical analysis of performance of a two-stage compression CO_2 cycle with two different evaporating temperatures.* Int. J. Refrig. **47**(2014), 164–175.

[18] Elakdhar M., Mehdi E., Kairouani L.: *Analysis of a compression-ejection cycle for domestic refrigeration.* Ind. Eng. Chem. Res. **46**(2007), 13, 4639–4644.

[19] Kairouani L., Elakhdar M., Nehdi E., Bouaziz N.: *Use of ejectors in a multi-evaporator refrigeration system for performance enhancement.* Int. J. Refrig. **32**(2009), 6, 1173–1785.

[20] Lin C., Cai W., Li Y., Yan J., Hu Y.: *Pressure recovery ratio in a variable cooling loads ejector-based multi-evaporator refrigeration system.* Energy **44**(2012), 1, 649–656.

[21] Lin C., Cai W., Li Y., Yan J., Hu Y., Giridharan K.: *Numerical investigation of geometry parameters for pressure recovery of an adjustable ejector in multi-evaporator refrigeration system.* Appl. Therm. Eng. **61**(2013), 2, 649–656.

[22] Lin C., Li Y., Cai W., Yan J., Hu Y., Gridharan K.: *Experimental investigation of the adjustable ejector in a multi-evaporator refrigeration system.* Appl. Therm. Eng. **61**(2013), 2–10.

[23] Zhou M., Wang X., Yu J.: *Theoretical study on a novel dual-nozzle ejector enhanced refrigeration cycle for household refrigerator-freezers.* Energy. Convers. Manag. **73**(2013), 278–284.

[24] Hafner A., Forsterling S., Banasiak K.: *Multi-ejector concept for R-744 supermarket refrigeration.* Int. J. Refrig. **43**(2014), 1–13.

[25] Chen L.T.: *A new ejector–absorber cycle to improve the COP of an absorption refrigeration system.* Applied Energy **30**(1988), 37–51.

[26] Nehdi E., Kairouani L., Bouzaina M.: *Performance analysis of the vapor compression cycle using ejector as an expander.* Int. J. Energ. Res. **31**(2007), 4, 364–375.

[27] Kairouani L., Elakhdar M., Nehdi E., Bouaziz N.: *Use of ejectors in a multi-evaporator refrigeration system for performance enhancement.* Int. J. Refrig. **32**(2009), 6, 1173–1185.

[28] Brunion O., Feidt M., Hive B.: *Compression of the working domains of some compression heat pumps and a compression-absorption heat pump.* Int. J. Refrig. **20**(1997), 5, 308–318.

[29] Cengel Y.A., Boles M.A.: *Thermodynamics: An Engineering Approach*, 6th Edn. McGraw-Hill, 2007.

[30] Bejan A.: *Advanced Engineering Thermodynamics.* John Wiley & Sons, 1998.

[31] Elias Bou Lawz Ksayer: *Étude et conception des systèmes á efficacité énergétique améliorée fonctionnant au CO_2 comme fluide frigorigène*. Chapt. 2, 2007.

[32] Huang B.J., Chang J.M., Wang C.P., Petrenko V.A.: *A 1-D analysis of ejector performance*. Int. J. Refrig. **22**(1999), 5, 354–364.